Heterogeneous Reactions of HOCl + HCl → Cl_2 + H_2O and $ClONO_2$ + HCl → Cl_2 + HN03 on Ice Surfaces at Polar Stratospheric Conditions

Liang T. Chu, Ming-Taun Leu and Leon F. Keyser

Earth and Space Sciences Division, Jet Propulsion Laboratory, California Institute of Technology, Pasadena, California 91109

Abstract

Heterogeneous reactions of HOCl + HCl → Cl_2 + H20 (1) and $ClONO_2$ + HCl → C12 + HN03 (2) on ice surfaces at a temperature of 188 K have been investigated in a flow reactor interfaced with a differentially pumped quadruple mass spectrometer. Partial pressures for HOCl and $ClONO_2$ in the range of 6.5 x 10-8 Torr to 2.0 x 10-6 Torr, which mimic conditions in the polar stratosphere, have been used. Uptake of HCl on ice surfaces using partial pressures of HCl in the range of 1.8 $x\ 10^{-7}$ Torr to 8.0 x 10-6 Torr has been measured prior to contact with HOCl or $ClONO_2$. Pseudo-first-order decays of HOCl and $ClONO_2$ over HCl-coated ice surfaces have been observed in all experiments under the conditions of $P_{HOCl} < P_{HCl}$ and $P_{ClONO2} < P_{HCl}$ used. Both the decay rates of HOCl and $ClONO_2$ and the growth rates of Cl_2 have been used to obtain reaction probabilities: γ_g (1) $\dot{=}$.34 ± 0.20 (la) and γ_g (2) = 0.27 ± 0.19 (1σ) if we assume that the area of ice surfaces is equal to the geometric area of the flow-tube reactor. By considering the morphology of ice films, we obtain true reaction probabilities γ_t(1) = 0.13 ± 0.08 and γ_t (2) = 0.103-0.08 using a previously published model of surface reaction and pore diffusion. In addition, the true reaction probability, γt (3), for the $ClONO_2 + H_2O$ → HOCl + HN03 (3) reaction has been measured to be greater than 0.03 on ice surfaces. Reaction mechanisms for these heterogeneous

reactions (1) - (3) are discussed, including a possible two-step mechanism for reaction (2) in terms of reaction (3) and reaction(1).

(to be submitted to the Journal of Physical Chemistry on)

hoclhcl.doc (07-12-93)

1. Introduction

It is now well established that heterogeneous reactions on the surfaces of polar stratospheric clouds (PSCs) are of vital importance in converting inactive chlorine to active forms which subsequently deplete ozone through catalytic cycles, such as ClO-ClO and BrO-ClO mechanisms, in the polar stratosphere [3]. These heterogeneous reactions include

$$HOCl + HCl \rightarrow C12 + H20 \quad (1)$$

$$ClONO_2 + HCl \rightarrow C12 + HN03 \quad (2)$$

$$ClONO_2 + H_2O \rightarrow HOCl + HN03 \quad (3)$$

Recent model calculations[4,5] have suggested that reaction (1) could be as important as reactions (2) and (3), particularly in the early Antarctic winter if $ClONO_2$ concentrations are lower than HOCl concentrations. Nevertheless, reaction (2) has been thought to comprise two elementary steps: the first step is reaction (3) followed by reaction (1)[6-8].

Reaction (1) on ice surfaces has been the subject of recent laboratory investigations. Abbatt and Molina[7] used an electron-impact ionization mass spectrometer (EIMS) interfaced to a flow reactor. These experiments were carried out at ice-film temperatures in the range 195-202 K and HCl partial pressures in the range 10^{-6} -10-5 Torr. Both temperatures and HCl partial pressures are significantly greater than those in the polar stratosphere (i. e., T = 180-188 K for type II PSCS and P_{HCl} = 10-8 -10-7 Torr). They reported a reaction probability γ_g (1) = 0.16 at 202 K and 0.24 at 195 K, respectively. A small negative temperature dependence was suggested. Hanson and Ravishankara[8] used a chemical ionization mass spectrometer (CIMS) for detection in a flow tube reactor and measured the first-order loss of HOCl on ice in the

presence of HCI partial pressures of 10-7-104 Torr. They reported $\gamma_g(1)$ for reaction (1) to be > 0.3 at 191 K. In these studies the surface area of the ice film was assumed to be equal to the geometric area of the flow reactor for the determination of γ_g (1); the internal surface area was not considered.

There are several laboratory studies of reactions (2) and (3). Some early investigations[9-11] are believed to suffer from surface deactivation by HN03 because higher reactant concentrations of $ClONO_2$ were used. Nevertheless, these studies were instrumental in demonstrating that heterogeneous reactions on PSCS surfaces are of importance in chlorine activation. Recently Hanson and Ravishankara[8,12] used CIMS with HCI partial pressures of 10-7-104 Torr. They reported a value of $\gamma_g = 0.3$ (+0.7, -O. 1) at 200 K for reactions **(2)** and (-3) on a surface consisting of NAT and ice. Another study was reported by Abbatt and Molina[6]. They used an EIMS apparatus and HCI partial pressures of 10-6- 10-5 Torr. They obtained γ_g (2) > 0.2 at 202 K for reaction (2) on a similar surface. Again, in these studies the geometric area was used to calculate the reaction probability.

In this work we report a new measurement of the reaction probability for reaction (1) at 188 K using partial pressures of reactants (10-8 - 10^{-6} Torr) similar to those in the polar atmosphere. Furthermore, we have reinvestigated reactions (2) and (3) using our new EIMS apparatus taking advantage of higher sensitivity detection. In the following sections we will briefly describe the experimental procedures used in the reaction probability determination and present our experimental results. We then discuss the effect of ice-film morphology on our results and compare them with previous measurements. Finally, a possible two-step mechanism for reaction (2) in terms of reaction (3) and reaction (1), and reaction mechanism for these heterogeneous reactions on ice surfaces are briefly discussed.

II. Experimental Section

The reaction probability measurement was performed in a flow reactor coupled to a differentially pumped quadruple mass spectrometer. The details of the apparatus have been discussed in our previous publications[13,14] and we will only briefly describe it in this article.

Flow Reactor. The flow reactor was constructed of borosilicate glass, and its dimensions are 1.76 cm inside diameter and 33.0 cm in length. The geometric area of the flow reactor is about 182.5 cm2. The temperature of the reactor was regulated by a refrigerated methanol circulator (Haake, Model FK2) and measured by a pair of thermocouples located in the middle and at the downstream end. During the experiment the temperature was maintained at 188 K. The accuracy of this measurement is about ± 0.5 K. The pressure inside the reactor was monitored by a high-precision pressure meter (MKS Instruments, Model 390 HS, 10 Torr full scale), which was located about 2 cm from the flow reactor at the downstream end.

Preparation of Ice Films. The ice film was prepared as follows: Helium carrier gas was bubbled through a water reservoir which was kept in a constant-temperature circulator, normally at 293 K, and the helium gas saturated with the water vapor was admitted to the inlet of the sliding Pyrex injector. During the period of deposition the sliding injector was slowly pulled out at a constant speed and an uniform ice film was deposited on the inner surface of the reactor, which was held at a temperature of 188K. After the ice film was prepared, the injector was kept at the upstream end in order to prevent warming of the substrate. The amount of ice substrate deposited was calculated from the water vapor pressure, the mass flow rate of the helium-water mixture (which was measured by a Hastings mass flow meter), and the deposition time. Some of the substrates were transferred to a U-tube at 77 K and weighed on an analytical balance. The results from these two methods are in good agreement.

Average film thickness was calculated by using the measured geometric area and weight of the deposit with a value of 0.63 g/cm^3 for the bulk density of vapor-deposited water ice[1] 5; the results ranged from 3.7 to 34.1 pm.

In addition, morphology of ice films was investigated under similar experimental conditions using an environmental scanning electron microscope 6 The results suggest that ice films comprise layers of micron-sized granules. This observation is in agreement with surface area measurements obtained by using BET analysis of gas-adsorption isothermal [5-17]. This information on the ice-film structure will be used to determine the true reaction probability in a later section.

HCl Mixtures and Uptake Measurements. HCl/He mixtures were prepared by mixing Matheson semiconductor-purity HCl (99.995 %) and Matheson-purity helium (99.9999 %) in a glass manifold which was previously evacuated to 10^{-6} Torr. Flow rates of the mixtures. were monitored by using a Hastings mass flowmeter. At first the He-HCl mixture was admitted to the flow reactor through an inlet located at the downstream end; this bypassed the ice film and allowed the vacuum lines to be conditioned with HCl. At the start of a typical uptake measurement, the flow was redirected through another inlet at the upstream end of the ice film. At saturation, the HCl uptake capacity on the ice surface based on the geometric area of the flow reactor was found to be 8 x 10^{14} to 1.1 x 10^{16} molecules/cm^2 depending on the partial pressure of HCl used, These results are reasonably consistent with our earlier observations[14].

HOCl Preparation and Calibration. The HOCl solution was prepared by mixing NaOCl with $MgSO_4 \cdot 7H_2O$[7,1] 9. Some modifications in the synthesis of HOCl were necessary in order to achieve a stable yield. We dissolved 40 g of $MgSO_4 \cdot 7H_2O$ in 75 ml of distilled water. Then we added the $MgSO_4$ solution to 75 ml of 6% NaOCl solution drop by drop in the dark. The solution was slowly stirred during the reaction in

which a white precipitate of $Mg(OH)_2$ was formed. After completing the synthesis, we separated the $Mg(OH)_2$ precipitate from the solution by recantation, A slightly yellowish clear HOCI (OCl^-) solution was obtained. Since HOCl is in equilibrium with ClO^- and H^+ in solution, it is very important to control the pH of the prepared solution in order to ensure that the equilibrium is shifted toward HOCI side. The pH of the solution should be close to neutral. By adding a small amount of dilute H2S04 to the HOCI solution, we were able to shift the equilibrium toward HOCI and increase the yield of the synthesis. The HOCI was further purified by vacuum distillation in order to decrease impurities such as, HCI, C12 and C120 which were checked by our mass spectrometer and were found to be smaller than 10 %.

Helium gas was bubbled through the HOCl solution which was maintained at 273 K. A small amount of water vapor (less than 1 % of the ice-film mass) from the HOCI solution was also admitted into the reactor. The water vapor was needed in order to prevent HOCI from decomposing into C120 by the reaction 2 HOCI $\rightarrow$ C120 + H20 during transport to the flow reactor. The concentration of gas-phase HOCl was calibrated by its production from $ClONO_2$ in reaction (3). For this we assume: (1) a stoichiometric ratio of unity for HOCI formed to $ClONO_2$ lost; and (2) no significant adsorption of HOCI on ice surface. In these experiments larger ice films were used in order to minimize deactivation by product HNO_3.

$ClONO_2$ synthesis and calibration. $ClONO_2$ was synthesized by mixing a small amount of C120 in N205 at 195 K the mixture was allowed to warm to 248 K to produce $ClONO_2$. This procedural [1,13] was repeated several times in order to prepare a sufficient amount of $ClONO_2$. The $ClONO_2$ thus prepared was further purified by vacuum distillation at 195 K and 178 K. The C12 impurity, which could interfere with our reaction probability measurements, was found to be small. Vapor pressures of $ClONO_2$ in the reservoir were measured by a high precision MKS pressure meter (MKS

Instruments, Model 390 HS, 1 Torr full scale).

Procedures for Reaction (1). The reaction probability of HOCl on an HCl-covered ice film was determined as follows. First, an ice film about 20 μm thick was prepared on the inner wall of the flow reactor. Second, the film surface was treated with HCl at pressures 9 x 10-7 to 8 x 10-6 Torr until its saturation uptake capacity was attained (see above). Then without turning off the HCl flow, HOCl at pressures between 1 x 10-7-2 x 10-6 Torr was admitted to the reactor. The loss rate of HOCl and the growth rate of Cl_2 were measured as a function of injector distance, z. The parent peaks of HOCl at m/e = 52 and of Cl_2 at m/e = 70 were used. Knowing the gas flow velocity, v, in the reactor, the reaction time was calculated by using f = z/v. The first-order rate constant, k_s, was calculated from the slope of a linear least-squares fit to the experimental data.(see next section) The gas-phase diffusion correction for k_s was made by using a standard procedure[20] and the corrected rate, k_g , was determined. The diffusion coefficient of HOCl in helium was estimated to be 193 Torr cm2 s^{-1} at 188 K[21]. Based on the geometric area of the flow-tube reactor the reaction probability, γ_g , was then calculated by using the following equation

$$\gamma_g = 2r_0k_g/(\varpi + r_0k_g) \quad (4)$$

where r_0 is the radius of the flow reactor (0,88 cm) and ϖ is the average molecular velocity for HOCl. In addition, correctional [7,18] were made for the interaction of surface reaction and pore diffusion to obtain the true reaction probability, γ_t. (see the following section).

Procedures for Reaction (2). The reaction probability for reaction (2) was measured in a manner similar to that used for reaction (1). Helium was bubbled through the $ClONO_2$ reservoir which was maintained at 155 K or lower, depending on

the $ClONO_2$ concentrations required in the experiment. The low temperature bath was prepared by mixing ethanol and liquid nitrogen. The helium gas saturated with $ClONO_2$ was introduced into the flow reactor. The $ClONO_2$ loss rate at m/e = **46** and the Cl_2 growth rate at m/e = 70 were measured as a function of injector distance. The procedures used to obtain reaction probabilities are identical to those used for reaction (1). The diffusion coefficient of $ClONO_2$ in helium was estimated to be 158 Torr cm2 s^{-1} at 188 K[13,21]. In addition, the reaction probability for reaction (3) was also measured on ice surfaces in the absence of an HCI coating.

Ill. **Results**

For an irreversible pseudo-first-order reaction under plug-flow conditions, the following equation holds for the reactant

$$\ln [St(z)] = -k_s(z/v) + \ln [St(0)] \quad (5)$$

where St is the signal, O is the reference injector position, v is the average flow velocity, and z is the injector position. The corresponding equation for the product signal, assuming rapid resorption and unit stoichiometry, is given by

$$\ln [St(z) - St(0)] = -k_s(z/v) + \ln [S_t(0) - S_t(\infty)] \quad (6)$$

where $S_t(\infty)$ is the signal when the reaction has reached completion. The left-hand sides of eqs (4) and (5) were plotted vs the" reaction time, z/v, for reactant decay and product growth, respectively. Observed reaction rate constants, ks, were obtained from linear-least-squares fits to these data.

HOCl + HCl → Cl_2 + H20. The reaction probability for this reaction was

measured by observing the decay of HOCl, monitored at m/e = 52 as a function of the injector position, In a separate run using the same ice film immediately after the HOCl decay measurement, the growth of Cl_2 at m/e = 70 was also monitored as a function of injector position. The thickness of the ice film was 19.4±0.4 μm and the temperature was 188 ± 0.5 K. Typical data are shown in Figure 1. The results from these experiments using P_{HOCl} in the range 1.3 x 10-7- 1.8×10^{-6} Torr and P_{HCl} in the range 9 x 10-7-8 x 10-6 Torr is summarized in Table I and also shown in Figure 2. Figure 2a shows the reaction probability, γ_g (1), determined from the loss rate of HOCl and Figure 2b illustrates the reaction probability measured from the growth rate of C12. The measured reaction probabilities presented in Figure 2 have been corrected for external gas-phase diffusion[20]. The average reaction probability is 0.30*0.18 from the decay rate of HOCl and 0.38±0.24 from the growth rate of C12. The overall average value of 41 experiments is $\gamma_g(1) = 0.34 \pm 0.20$. The uncertainty represents one standard deviation (1a). The results are approximately independent of P_{HOCl} and P_{HCl}. (see next section for detailed discussion) In addition, the Cl_2 yield based on HOCl reacted has been measured to be 0.80 ± 0.20.

Several experiments were also carried out in the absence of an HCl-coating on ice surfaces. The first-order rate constant of the HOCl decay is much smaller than that reported in the previous paragraph. Furthermore, no reaction products were observed in these experiments.

$ClONO_2 + HCl \rightarrow Cl_2 + HNO_3$. The reaction probability for reaction (2) was determined in the same manner as that for reaction (1). Typical data are shown in Figure 3. The decay of $ClONO_2$ was monitored by its major fragment peak m/e = 46 while the reaction product, Cl_2, was measured by its parent peak m/e = 70. The concentration of HCl used in the investigation is always greater than that of $ClONO_2$, thus a first-order rate constant can be calculated from the observed decay. We have

varied P_{ClONO_2} in the range 6.5x10-8 Torr - 9.7×10^{-7} Torr and P_{HCl} from 1.6×10^{-7} Torr to 2.3x10-6 Torr. The ice film thickness was about $10.4\pm1.3\,\mu m$ and the temperature was 188 ± 0.5 K. These data are summarized in Table II and also shown in Figures 4a and 4b. Some of data indicate that γ_g (2) may be greater at higher HCl partial pressures. However, the overall measured reaction probability γ_g (2) seems to be nearly independent of P_{ClONO_2} and P_{HCl} after considering the uncertainty of the measurements. (see next section for detailed discussion) We obtain an average γ_g = 0.26 ± 0.19 from the decay rate of $ClONO_2$ and γ_g = 0.28 ± 0.18 from the growth rate of C12. The overall average reaction probability of 24 experiments is γ_g (2) = 0.27 ± 0.19. The uncertainty represents one standard deviation (1σ). In addition, the C12 yield based on the $ClONO_2$ reacted has been measured to be 1.2 ± 0.2.

$ClONO_2$ + H20 → HOCl + HNO_3. We have also remeasured the reaction probability for the reaction of $ClONO_2$ + H20 → HOCl + HN03 on ice surfaces. As noted in the Introduction Section, the ice is readily contaminated by the reaction product, HNO_3, which forms a thin layer of hydrated nitric acid (possibly nitric acid trihydrate, NAT) on the surface. Therefore a very small reactant concentration of $ClONO_2$ about 1.4 x 10-7 Torr was used in these experiments. The results are summarized in Table Ill. In every experiment we first measure the $ClONO_2$ decay and then measure the growth of the HOCl signal. In general, the data obtained from the HOCl growth is equal to or smaller than that obtained from the $ClONO_2$ decay because of surface deactivation by product HN03. If the geometric area of the flow-tube reactor is used to obtain the reaction probability, γ_g (3) ranges from 0.03 on thinner ice films to 0.13 on thicker ice films.

IV. **Discussion**

Correction for the morphology of ice films.

A model taking surface reaction and pore diffusion into account has been described recently.[17,18] Based on observations using environmental scanning electron microscopy,[16] H20 ice films can be described in terms of a model consisting of hexagonally close-packed (HCP) spherical granules stacked in layers. In this case the true reaction probability, γ_t, is related to the value, γ_g, by

$$\gamma_t = \gamma_g \pi^{-1} 3^{1/2} \{1+\eta[2(N_L-1)+ (3/2)^{1/2}]\}^{-1} \quad (7)$$

where η is the effectiveness factor, and $N_L = 2 + 9 \log_{10} h(\mu m)$ is the number of granule layers and h is the film thickness. Using this model, we obtain the following true reaction probabilities: γ_t (1) = 0.13 ± 0.08 for reaction (1) and γ_t (2) = 0.10 ± 0.08 for reaction (2).

The model includes corrections for external surface roughness and for internal porosity. Roughness is defined as the ratio of total external surface area to the area of the underlying substrate. For the layer model, the surface roughness has a value of about 2. The overall correction to γ_g for reactions (1) and (2) is about a factor of 2.6; thus, most of the correction is due to the surface roughness. This is consistent with the fact that at high γ_t (> 0.1) gas-phase diffusion of HOCl and $ClONO_2$ into the porous film cannot compete with reaction at the external surface and most of the internal film surface does not participate in the reaction, [17] For $\gamma_t > 0.1$, surface roughness still should be considered, even though the mean free path of the reacting gas is greater than the dimensions of the roughness.[22,23] Under flow-reactor conditions, the velocity distribution directed at the surface is almost random; moreover, after the first collision for γ_t c 1, the gas molecules leave the surface with completely random velocities and can undergo secondary collisions with the surface. In effect, after the first collision the

reacting gas becomes partially trapped within the surface irregularities. Thus, even for long mean free paths almost the entire external surface can be sampled.

A similar treatment used to obtain true reaction probabilities for reactions (l') and (2) can be applied to the data (Table Ill) for reaction (3). An average value γ_t (3) = 0.03 was found. This value should be considered as a lower limit because of surface deactivation by product HN03.

Comparison with previous measurements.

In Figure 5 we compare our data of $\gamma_g(1)$ with previous measurements of reaction (1) reported by Abbatt and Molina[6] and Hanson and Ravishankara[8]. These data are not corrected for the internal surface area of ice films. Our measurement is in good agreement with these recent data. There is a possibility that a slight negative temperature dependence for reaction (1) may exist. However, within uncertainties of these measurements $\gamma_g(1)$ should be considered to be nearly independent of, temperature.

Similarly, our present data on reaction (2), γ_g (2), is compared with the previous measurements which are shown in Figure 6. Our present measurement is in excellent agreement with the recent data reported by Abbatt and Molina[7], and Hanson and Ravishankara8. Again, γ_g (2) should be considered to be nearly independent of temperature within uncertainties of these measurements.

For reaction (3), surface deactivation by product HN03, which may form hydrates of nitric acid, reduces $\gamma_t(3)$. Therefore, this value should be considered as a lower limit. This measurement is consistent with the recent data, γ_g (3) = 0.2-1.0, reported by Hanson and Ravishankara[8,12,24].

Reaction Mechanism.

It has been suggested that reaction (2) may proceed through reaction (3) and then reaction (1)6-8, This is an intriguing question which needs to be resolved. From

our measurements reported in the previous section, $\gamma_g(3)$ could be smaller than $\gamma_g(1)$; and thus, it could serve as a rate limiting step. Furthermore, in our experiments $\gamma_g(2)$ is also greater than $\gamma_g(3)$. Therefore, although the two-step mechanism is possible, a direct reaction between $ClONO_2$ and HCl could be more important than the two-step mechanism, Abbatt and Molina[7] also reached the same conclusion in their study of these reactions on a NAT surface.

Adsorption isotherms have been used to discuss these heterogeneous reactions on ice surfaces.[25-28] For reaction (1), since the adsorption equilibrium constant, b_{HOCl}, for HOCl is smaller than that for HCl, b_{HCl}, and $P_{HOCl} < P_{HCl}$, thus the $b_{HOCl}P_{HOCl}$ term can be neglected as compared with the $b_{HCl}P_{HOCl}$ term. Also, HCl molecules on ice surfaces dissociate into H^+ and Cl^-.[29-31] Based on the Langmuir isotherm, an equation for the relationship between γ_g and P_{HCl} is given as follows

$$\gamma_g = \gamma_o \theta_{HCl} = \frac{\gamma_o (b_{HCl}P_{HCl})^{1/2}}{[1 + (b_{HCl}P_{HCl})^{1/2}]} \qquad (8)$$

where γ_o is the reaction probability on an ice surface at its saturation capacity for HCl. This equation predicts that γ_g increases linearly with $P_{HCl}^{1/2}$ at low HCl pressures and becomes nearly independent of P_{HCl}^{1} /2 at pressures where the surface is saturated with HCl. Our results in Figures 2(a) and 2(b) show that γ_g increases with P_{HCl} at low P_{HOCl} as predicted by eq (8). However, the results in Figures 2(c)-(f) at higher P_{HOCl} show that within experimental uncertainties γ_g is nearly independent of P_{HCl}, this suggests that during these experiments the ice surfaces are nearly saturated with HCl over the pressure range used in this study. It is worthwhile to note that the

experimental technique used in this work is not particularly sensitive to γ_g greater than 0.2, Also, the formation of hydrogen hexahydrate or melting takes place on ice surfaces at P_{HCl} greater thar 1×10^{-5} Torr. In order to validate this mechanism, more accurate measurements for reaction (1), perhaps using a different experimental approach over wide range of eactant concentrations, are needed, Similarly, we reach the same conclusion for reaction (2), The results for this reaction are shown in Figures 4(a)-(d).

Molina[29] has suggested an ionic mechanism for these heterogeneous reactions on ice surfaces; for example, reaction (1) can be depicted as

$$\begin{array}{lcl} & \text{ice} & H^+ \; Cl^- \\ HC + HOCl \rightarrow & & H\;O^-\;Cl^+ \rightarrow Cl_2\,(g) + H20\,(S) \end{array} \qquad (9)$$

In this mechanism a quasi-liquid layer could be formed after the solvation of HCl on ice surfaces even at stratospheric conditions: T = 180-200 K and P_{HCl} = 10-7 Torr. The dissociation of HCI on ice surfaces has been suggested in our previous article[1]3 and elsewhere[29-31]. This suggestion is very intriguing because mobility of HCI in the liquid is much greater than that in solid ice by several orders of magnitude. Therefore, HCI molecules would be readily available for reaction with HOCl. However, there is a question about the dissociation of HOCl forming HO^- and Cl^+ (or possibly H^+ and ClO^-) in a quasi-liquid layer. In addition, the existence of this quasi-liquid layer under polar stratospheric conditions has been questioned.27 Further investigation on single-crystal ice as proposed by Kroes and Clary[27] is certainly required.

Conclusion

In summary, the present investigation has been performed under experimental

conditions which mimic the polar environment, such as, temperature, ice substrate, and reactant concentrations. Therefore, the results are directly applicable to atmospheric modelling. The time constant in converting inactive chlorine to active forms on the basis of our reaction probability measurements and estimated surface area for Type II PSCS is about a few hours in the wintertime polar stratosphere.32

Acknowledgments

The research described in this article was performed at the Jet Propulsion Laboratory, California Institute of Technology, under a contract with the National Aeronautics and Space Administration.

Reference

1. *Scientific Assessment of Ozone Depletion: 1991*; World Meteorological Organization Global Ozone Research and Monitoring Project, Report No. 25.
2. Kolb, C. E.; Worsnop, D. R.; Zahniser, M. S.; Davidovits, P.; Hanson, D. R.; Ravishankara, A. R.; Keyser, L. F.; Leu, M-T.; Williams, L. R.; Molina, M. J.; Tolbert, M. A. in *Current Problems in Atmospheric Chemistry,* edited by J. R. Barker, in press, World Scientific Publishing Company (1 993).
3. Solomon, S. *Nature*, **1990**, 347,347.
4. Prather, M. J. *Nature*, *1992, 355,534.*
5. Crutzen, P. J.; Muller, R.; Bruhl, Ch.; Peter, Th. *Geophys. Res. Lett.* **1992, *19*, 1113!**
6. Abbatt, J. P. D.; Molina, M. J. *J. Phys. Chem. 1992, 96, 7674.*
7. Abbatt, J. P. D.; Molina, M. J. *Geophys. Res. Lett.* **1992, *19*, 461.**
8. Hanson, D. R.; Ravishankara, A. R. *J. Phys. Chem. 1992, 96, 2682.*
9. Molina, M. J.; Tso, T. L.; Molina, L. T.; Wang, F. C. Y. *Science,* **1987, 238, 1253.**
10. Tolbert, M. A.; Rossi, M. J.; Malhotra, R.; Golden, D. M. *Science,* **1987**, *238, 1258.*
11. Leu, M-T., *Geophys. Res. Lett.* 1988, *15*, 17.
12. Hanson, D. R.; Ravishankara, A. R. *J. Geophys. Res.* **1991, 96, 5081,**
13. **Leu,** M-T.; Moore, S. B.; Keyser, L. F. *J. Phys. Chem. 1991, 95, 7763.*
14. Chu, L. T.; Leu, M-T.; Keyser, L. F. *J. Phys. Chem.*, in press, 1993.
15. Keyser, L. F.; Leu, M-T. *J. Colloid Interface Sci.* **1993**, *155*, *'137,*
16. Keyser, L. F.; Leu, M-T. *Microscopy Res. Technique,* in press, 1993.
17. Keyser, L. F.; Moore, S. B.; Leu, M-T. *J. Phys. Chem. 1991, 95,5496.*
18. Keyser, L. F.; Leu, M-T.; Moore, S. B. *J. Phys. Chem. 1993, 97,2800.*

19. D'Ans, J.; Freund, H. E. Z, *Elekrtochem. 1957, 61*, 10.

20. Brown, R. L, *J. Res. Nat/. Bur. Stand. (U. S,), 1978, 81, 1.*

21. Marrero, T. R.; Mason, E. A. *J. Phys. Chem. Ref. Data, 1972, 1*, 3.

22. Takaishi, T. *J. Phys. Chem.* 1957, *61*, 1450.

23. McKee, C. S.; Roberts, M. W. Trans. Faraday Sot. 1967, 63, 1418,

24. Hanson, D. R.; Ravishankara, A. R. *J. Phys. Chem.* 1993, 97,2802.

25. Elliot, S.; Turco, R. P,; Toon, O. B.; Hamill, P. *J. Atmos. Chem.* **1991, *13*, 211.**

26. Mozurkewich, M. *Geophys. Res. Lett. 1993, 20, 355.*

27. Kroes, G-J.; Clary, D. C. *J. Phys. Chem.* **1992**, *96, 7079.*

28. Tabazadeh, A.; Turco, R. P. *J. Geophys. Res.* **1993**, in press.

29. Molina, M. J. in *CHEMRA WN VII: Chemistry of the atmosphere: The impact of global change,* J. G. Calvert, Ed. (Blackwell Sci. Publ., Oxford, in press).

30. Hanson, D. R.; Mauersberger, K. *Geophys. Res. Lett.* 1988, *15*, 1507.

31. Hanson, D. R.; Mauersberger, K, *J. Phys. Chem. 1990, 94,4700.*

32. Turco, R. P.; Toon, O. B.; Hamill, P. *J. Geophys. Res.* **1989**, 94, 16493,

Table I. Reaction Probability for the reaction of HOCl + HCl → Cl_2 + H_2O on ice surfaces.

P_{HOCl} (Torr)	P_{HCl} (Torr)	*Thickness* (μm)	HOCl Decay			Cl_2 Growth		
			k_s^a (1/s)	k_g^b (1/s)	γ_g^c	k_s^a (1/s)	k_g^b (1/s)	γ_g^c
1.1×10	2.82×10	19.5	1.18×10	5.83×10	0.25	1.18×10	3.83×10	0.25
1.2×10	1.11×10	19.6	1.74×10	3.74×10	0.10	0.17×10	1.86×10	0.12
1.4×10	2.27×10	19.4	1.26×10	3.48×10	0.20	1.29×10	4.99×10³	0.31
1.5×10	2.84×10⁻⁶	19.5	1.36×10³	4.52×10³	0.25	1.37×10³	6.77×10³	0.40
1.5×10	1.62×10⁻⁶	19.2	1.42×10³	4.97×10³	0.27	9.98×10²	2.24×10³	0.15
1.6×10	9.38×10	19.9	1.03×10³	2.16×10	0.13	0.11×10	1.86×10³	0.13
2.1×10	1.11×10	19.6	1.07×10	2.31×10	0.14	1.22×10³	2.85×10³	0.25
2.2×10	1.13×10	19.6	1.09×10	2.39×10	0.14	1.03×10⁵	2.42×10³	0.16
2.6×10	2.84×10	19.5	1.32×10	4.14×10	0.23	1.57×10⁵	2.34×10⁴	0.93
2.6×10	2.27×10	19.4	1.27×10	3.58×10	0.21	1.02×10³	2.40×10³	0.16
2.8×10	1.62×10⁻⁶	19.2	1.21×10³	3.08×10³	0.18	0.27×10²	1.02×10³	0.13
2.9×10	3.02×10	19.2	1.19×10	3.04×10	0.18	1.82×10³	>3×10⁴	1.0
3.2×10	2.27×10	19.4	1.19×10⁵	3.01×10³	0.18	1.15×10³	3.30×10³	0.22
3.3×10	1.12×10⁻⁶	19.6	1.05×10³	2.24×10³	0.13	8.25×10²	1.52×10³	0.11
3.3×10	9.31×10	19.9	1.22×10	3.16×10	0.18	1.16×10³	3.38×10³	0.22
3.9×10	2.84×10⁻⁶	19.5	1.28×10³	3.76×10³	0.21	1.26×10³	4.70×10³	0.30
4.0×10	1.63×10	19.2	1.04×10	2.20×10	0.13	1.71×10³	>3×10⁴	1.0
4.8×10	2.26×10	19.4	1.61×10	9.39×10	0.46	8.29×10²	1.54×10³	0.11
5.0×10	1.14×10⁻⁶	19.6	1.45×10³	5.33×10³	0.29	1.15×10³	3.26×10³	0.21
5.2×10	4.65×10⁻⁶	19.1	1.36×10	4.63×10	0.26	1.30×10³	5.39×10³	0.33
5.3×10	9.22×10	19.9	1.44×10	5.41×10	0.29	1.39×10³	6.80×10³	0.40
5.5×10	2.83×10⁻⁶	19.5	1.51×10	7.13×10	0.37	1.41×10³	8.30×10³	0.47
5.8×10	4.23×10⁻⁶	19.9	1.75×10	1.86×10	0.74	9.17×10²	1.94×10³	0.13

5.9 X10-7	2.27×10^{-6}	19.4	I.04X10^{3}	2.22X10^{3}	0.13	1.43×10^{3}	8.53×10^{3}	0.48
6.3x10^{-7}	1.62x10^{4}	19.2	1.57X10^{3}	7.91×10^{3}	0.40	1.36x10^{3}	6.12x10^{3}	0.37
7.0 X10-7	4.65x10^{4}	19.1	1.44X 103	5.70×10^{3}	0.31	1.53X1(Y	1.63x10^{4}	0.75
7.1 X10-7	1.13X10^{4}	19.6	1.70×10^{3}	I.27x10^{4}	. 0.58	1.20×10^{3}	3.70X10^{3}	0.24
7.1X10^{7}	1.69×10^{-6}	19.8	1 .40X 10^{3}	4.95X 103	0.27	1.49X 103	1.04×10^{4}	0.55
8.1x10^{-7}	2.10X10^{4}	19.9	1.63x10^{3}	I.02X10^{4}	0.49	1.31X10^{3}	5.24×10^{3}	0.32
8.8X10^{7}	9.24x10^{-7}	19.9	1.30×10^{3}	3.87x10^{3}	0.22	1.37×10^{3}	6.52×10^{3}	0.39
9.9 X10-7	1.65×10^{-6}	19.2	1.39X 103	4.74X 103	0.26	1.38x 103	6.62x 103	0.39
1 .0×10^{-6}	4.65x10^{X}	19.1	9.95X10^{2}	2.05x10^{3}	0.12	1.31X10^{3}	5.62x10^{3}	0.34
1.1X10^{4}	4.65×10^{-6}	19. I	1.40X 103	5.13X10^{3}	0.28			
1.3×10^{-6}	1.35×10^{-6}	20. I	I. SOX10^{3}	2.86x 104	0.95	9.53X10^{2}	2.07×10^{3}	0.14
1.3×10^{-6}	1.38x 10X	18.5	1.50X10^{3}	6.50x 103	0.34	1.33X10^{3}	5.67×10^{3}	0.35
1.3X10^{4}	3.46x 10A	19.9	1.44X10^{3}	5.45×10^{3}	0.30	9.41X 102	2.02X 103	0.14
1.7×10^{-6}	2.10×10^{-6}	18.4	1.31×10^{3}	4.09X 103	0.23	1.37X10^{3}	7.00X 103	0.41
1.7X10^{4}	4.31×10^{-6}	19.2	1.33×10^{3}	4.19X 103	0.24	1.49X10^{3}	1.13X10^{4}	0.5s
1.8×10^{-6}	1.43X10^{4}	19.4	1.57X10^{3}	8.61X10^{3}	0.43	1.34×10^{3}	6.05x10^{3}	0.36
1.8×10^{-6}	7.97X10^{4}	18.1	1.75X10^{3}	2.11X10^{4}	0.80	1.52x10^{3}	I.42x10^{4}	0.69
2.0×10^{-6}	1.76×10^{-6}	18.7	1.34×10^{3}	4.41×10^{3}	0.25			

Notes:

a Obtained from eq 5.

b After correction for gas-phase axial and radial diffusion, see Ref 20.

c Obtained from eq 4 which is based on the geometric area of the flow reactor.

d Obtained from eq 6.

Table II. Reaction probability for the reaction of $ClONO_2 + HCl \rightarrow Cl_2 + HNO3$ on NAT/ice surfaces.

P_{ClONO_2} (Torr)	P_{HCl} (Torr)	*Thickness* (μm)	C1ONO2 Decay			Cl_2 Growth		
			k_s^a (1/s)	k_g^b (1/s)	γ_g^c	k_s^d (1/s)	k_g^b (1/s)	γ_g^c
6.5×10^{-8}	$9.95X10^{7}$	9.8	$I.48x10^{3}$	$I.45X10^{4}$	0.77	$I.40X10^{3}$	$7.57X10^{3}$	0.44
$6.5x10^{4}$	7.54 X10-7	9.5	6.84×10^{2}	1.13×10^{3}	0.094	$I.16x10^{3}$	3.43X1(Y	0.22
$6.6X10^{-8}$	$6.67x10^{-7}$	9.9	1.51×10^{3}	$I.57X10^{4}$	0.81	$I.35X10^{3}$	$5.88x10^{3}$	0.36
6.7x 10$	$4.36x10^{-7}$	10.0	$1.10X10^{3}$	$3.09X10^{3}$	0.24	$8.15x10^{2}$	$1.52x10^{3}$	0.11
6.7×10^{-8}	3.29×10^{-7}	10.6	$9.29x10^{2}$	$2.01X10^{3}$	0.16	1.44x 10^{3}	8.62x 103	0.48
$6.9x10^{-8}$	$2.82x10^{-7}$	9.9	$9.51X10^{2}$	$2.13x10^{3}$	0.17	9.04X 102	$1.85x10^{3}$	0,13
$1.3X10^{7}$	8.12×10^{-7}	12.3	1.03X 103	2.66x 10^{3}	0.21	$1.37X10^{3}$	5.90X 103	0.36
1.4×10^{-7}	$I.24x10^{4}$	10.1	1.40X 103	$9.61x10^{3}$	0.59	$1.54X10^{3}$	$1.96x10^{4}$	0.84
1.4×10^{-7}	1.64 X10-7	9.6	$7.47X10^{2}$	1.33×10^{3}	0.11			
1.4 X10"^{7}	$2.68x10^{7}$	9.5	$8.23x10^{2}$	$I.61x10^{3}$	0.13	$7.79X10^{2}$	$1.42x10^{3}$	0.10
1.4 X10-7	5.05×10^{-7}	12.5	$8.41x10^{2}$	$1.64X10^{3}$	0.13			
1.5 X10-7	1.78×10^{-7}	9.8	$8.26x10^{2}$	$I.62x10^{3}$	0.13			
1.5 X10-7	$1.78x10^{-7}$	11.4	$9.13X10^{2}$	$I.95X10^{3}$	0.16			
$1.5X10^{7}$	3.44X 107	12.4	$7.36x10^{2}$	$1.29x10^{3}$	0.11			
1.5X10 ^{7} I	3.73X10^{7} I	9.7	$8.75x10^{2}$	$1.84x10^{3}$	0.15	7.57×10^{2}	$1.36x10^{3}$	0.096
3.1X10 ^{7} I	4.59 X10-7 I	9.3	$1.00x10^{3}$	$2.50x10^{3}$	0.20	$9.37x10^{2}$	2.05×10^{3}	0.14
3.1 X10-7	1.0 2x1 0 ^{4}	9.2	$1.06x10^{3}$	3.00×10^{3}	0.23	$1.34x10^{3}$	7.16×10^{3}	0.42
$3.2x10^{-7}$	6.47x 107	9.4	$1.23x10^{3}$	$4.76x10^{3}$	0.34	1.19X 103	3.90X 103	0.25
$3.2x10^{-7}$	$1.34X10^{4}$	9.3	$9.44X10^{2}$	$2.21X10^{3}$	0.18	$9.54X10^{2}$	2.19x 103	0.15
$3.2x10^{-7}$	$8.36x10^{7}$	9.5	8.07x 102	$1.57X10^{3}$	0.13	$1.24x10^{3}$	$4.68x10^{3}$	0.29
9.6x10 $^{-7}$	$9.06x10^{-7}$	9.7	$I.18x10^{3}$	$4.04x10^{3}$	0.30	8.98x10 ^{2}	1.86x1o^{3}	0.13

9.6×10^{-7}	1.23×10^{-6}	9.4	$1.11X10^{3}$	$3.29x10^{3}$	0.25	$9.10XI0^{2}$	1.92x 103	0.13
9.7 X10-7	1.84×10^{-6}	9.9	$1.11X10^{3}$	$3.48x10^{3}$	0.26	$1.23x10^{3}$	$4.65x10^{3}$	0.29
9.7 X10-7	$2.33x10^{6}$	9.3	9.09X 102	2.04x 103	0.16	9.09X 102	$4.86x10^{3}$	0.30

Notes:

[a] Obtained from eq 5.

b After correction for gas-phase axial and radial diffusion, see Ref 20.

c Obtained from eq 4 which is based on the geometric area of the flow reactor.

d Obtained from eq 6.

Table III. Reaction Probability of $ClONO_2$ + H20 → HOCl + HNO_3 on NAT/Ice surfaces.

P_{ClONO_2} (Torr)	*Thickness* (μm)	$ClONO_2$ Decay			HOCl Growth		
		k_s^a (1/s)	k_g^b (1/s)	γ_g^c	k_s^d (1/s)	k_g^b (1/s)	γ_g^c
I .45x 10-7	3.7	4.33X102	5.74×10²	0.05	3.64×10²	4.48×10²	0.03
1.44 X10-7	4.2	6.78×10²	1.10×10³	0.09	6.14x 102	8.91x102	0.06
1.46x 10-7	8.6	7.75×10²	1.39X103	0.13	5.28×10²	7.25x102	0.05
I.21X10-7	9.0	5.43X102	7.82×10²	0.07	7.80×10²	1.34X103	0.08
1.43 X10-7	9.2	6.50x 102	1. O3X103	0.09	8.74x 102	1.56x 10³	0.10
I.45X10-7	10.6	7. O3X102	I.18x103	0.10	7.54×10²	1.22×10³	0.08
1.42x10-7	18.9	7.35×10²	1.26×10³	0.10	8.83×10²	1.58×10³	0.10
1.21 X10-7	24.8	8.49x 102	1.64X103	0.13	9.16×10²	1.69x10³	0.10
1.42×10-7	25.7	8. I1x102	1.50×10³	0.12			
1.42x10-'	34.1	6.93x102	1.14X103	0.10			

Notes:

a Obtained from eq 5.

b After correction for gas-phase axial and radial diffusion, see Ref 20.

c Obtained from eq 4 which is based on the geometric area of the flow reactor.

d Obtained from eq 6.

Figure Captions

Figure 1. The HOCl decay and the Cl_2 growth in the reaction of HOCl + HCl $\rightarrow$ Cl_2 + H_2O on ice surface, The experimental conditions are: P_{total} = 0.398 Torr, v = 1720 cm/s, P_{HOCl} = 8.1 x 10-7 Torr, P_{HCl} = 2,1 x 10^{-6} Torr, h = 19.9 μm, and T = 188 K.

Figure 2. Summary of the data for the reaction of HOCl + HCl $\rightarrow$ Cl_2 + H20 on ice surfaces. The data shown in this figure is the average value of the data obtained both 'from the HOCl decay rates and from the Cl_2 growth rates. Partial HOCl pressures are: (a) 1.3 x 10-7 Torr, (b) 2.9 x 10-7 Torr, (c) 5.6x 10-7 Torr, (d) 7.3x 10-7 Torr, (e) 1.2x 10^{-6} Torr, and (f) 1.8 x 10-6 Torr. See Table I for detailed experimental conditions.

Figure 3. The $ClONO_2$ decay and the Cl_2 growth in the reaction of $ClONO_2$ + HCl $\rightarrow$ Cl_2 + HN03 on a surface consisting ice and NAT, The experimental conditions are: P_{total} = 0.400 Torr, v = 1730 cm/s, P_{ClONO2} = 1.4 x 10-7 Torr, P_{HCl} = 5.1 x 10-7 Torr, h = 12.5 μm, and T = 188 K.

Figure 4. Summary of the data for the reaction of $ClONO_2$ + HCl $\rightarrow$ C12 + HN03 on NAT/ice surfaces. The data shown in this figure is the average value of the data obtained both from the $ClONO_2$ decay rates and from the Cl_2 growth rates, Partial $ClONO_2$ pressures are: (a) 6.6x 10-8 Torr, (b) 1,4x 10-7 Torr, (c) 3.1 x 10-7 Torr, and (d) 9.7 x 10-7 Torr. See Table II for detailed experimental conditions.

Figure 5. Comparison of the present reaction probability data with previous measurements for the reaction of HOCl + HCl $\rightarrow$ C12 + H20 on ice surfaces. ❑ this work; A Hanson and Ravishankara8 ; O Abbatt and Molina[6]. See text for details.

Figure 6. Comparison of the present reaction probability data with previous

measurements for the reaction of $ClONO_2 + HCl \rightarrow$ C12 + HN03 on NAT/ice surfaces. □ this work; A Hanson and Ravishankara[8,12]; O Abbatt and Molina[7]. See text for details.

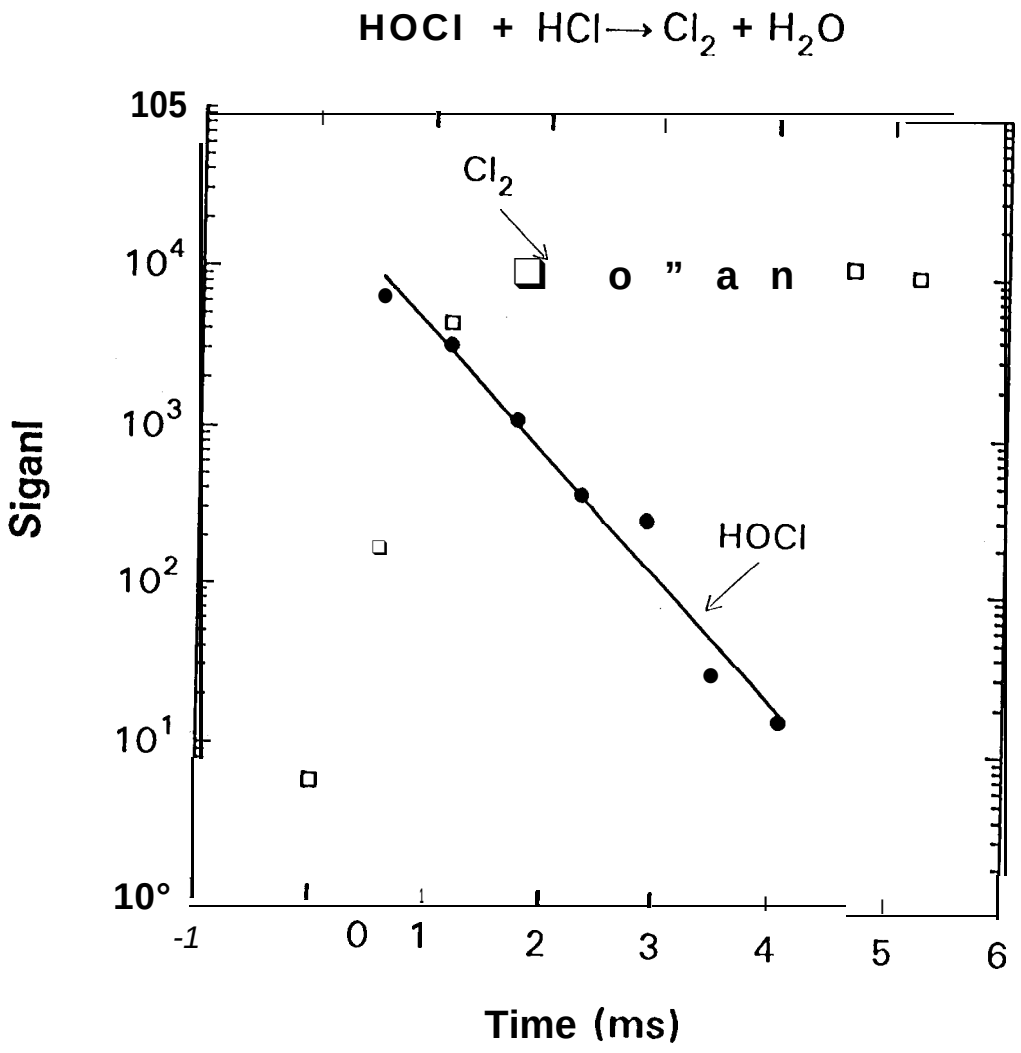
HOCl + HCl → Cl2 + H2O
105
10^4
10^3
10^2
10^1
10°
Siganl
Cl2
HOCl
-1
0
1
2
3
4
5
6
Time (ms)

Figure 1

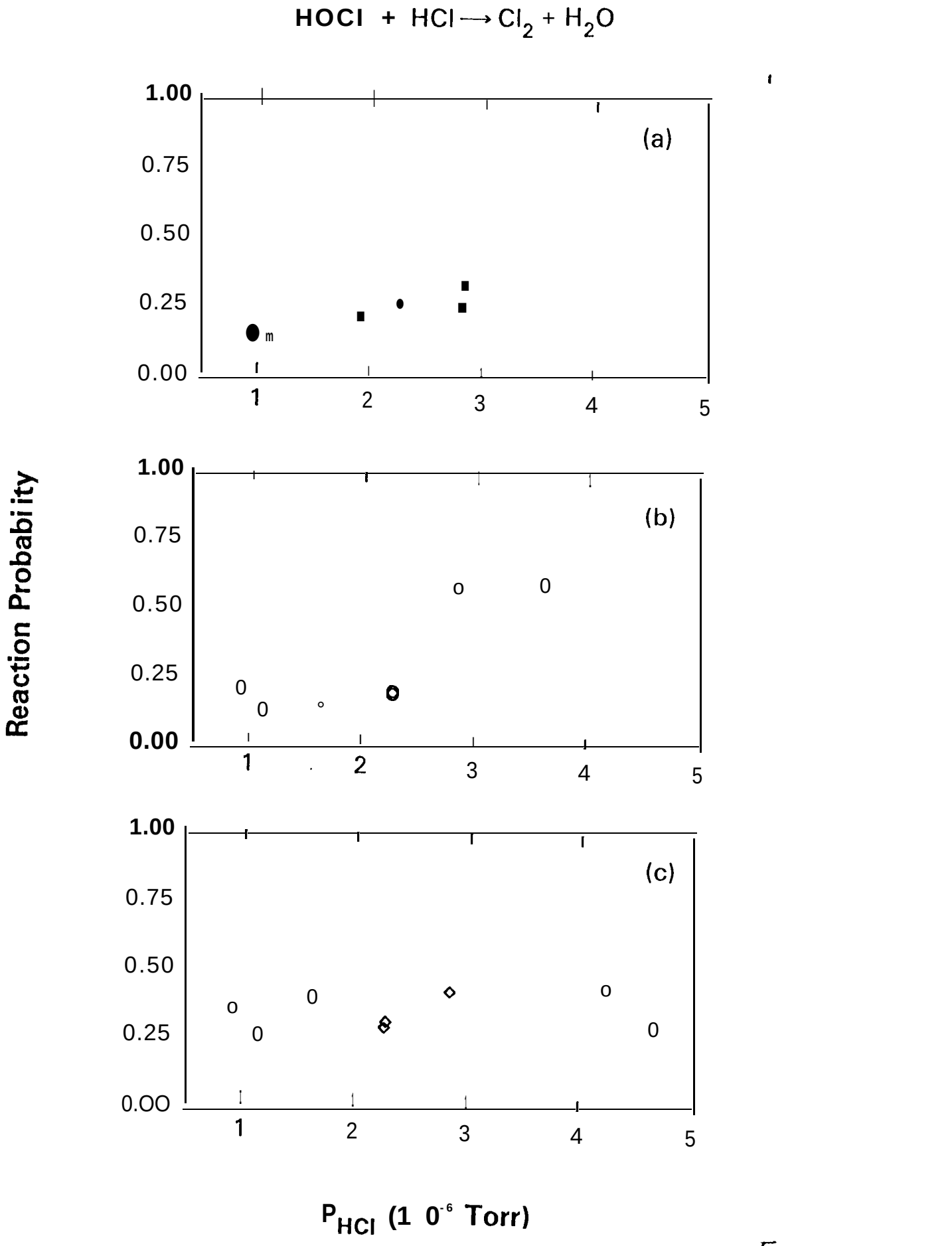

HOCISEP1.SP5

Figures 2(a)-(c)

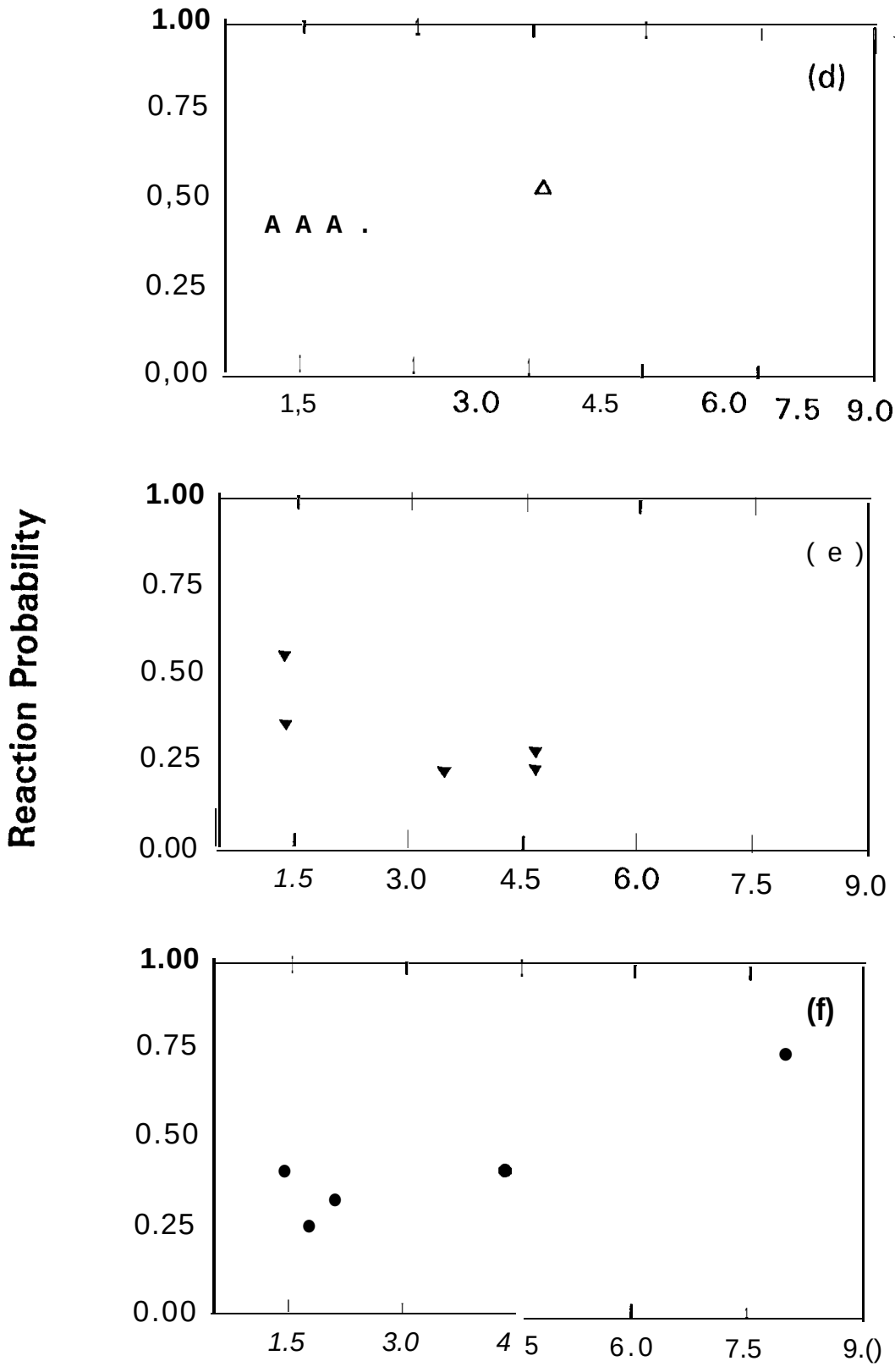
1.00
0.75
0,50
0.25
0,00
(d)
1,5
3.0
4.5
6.0
7.5
9.0
1.00
0.75
0.50
0.25
0.00
(e)
1.5
3.0
4.5
6.0
7.5
9.0
1.00
0.75
0.50
0.25
0.00
(f)
1.5
3.0
4 5
6.0
7.5
9.()
Reaction Probability
P HCl (1 0 - 6 Torr)

Figures 2(d)-(f)

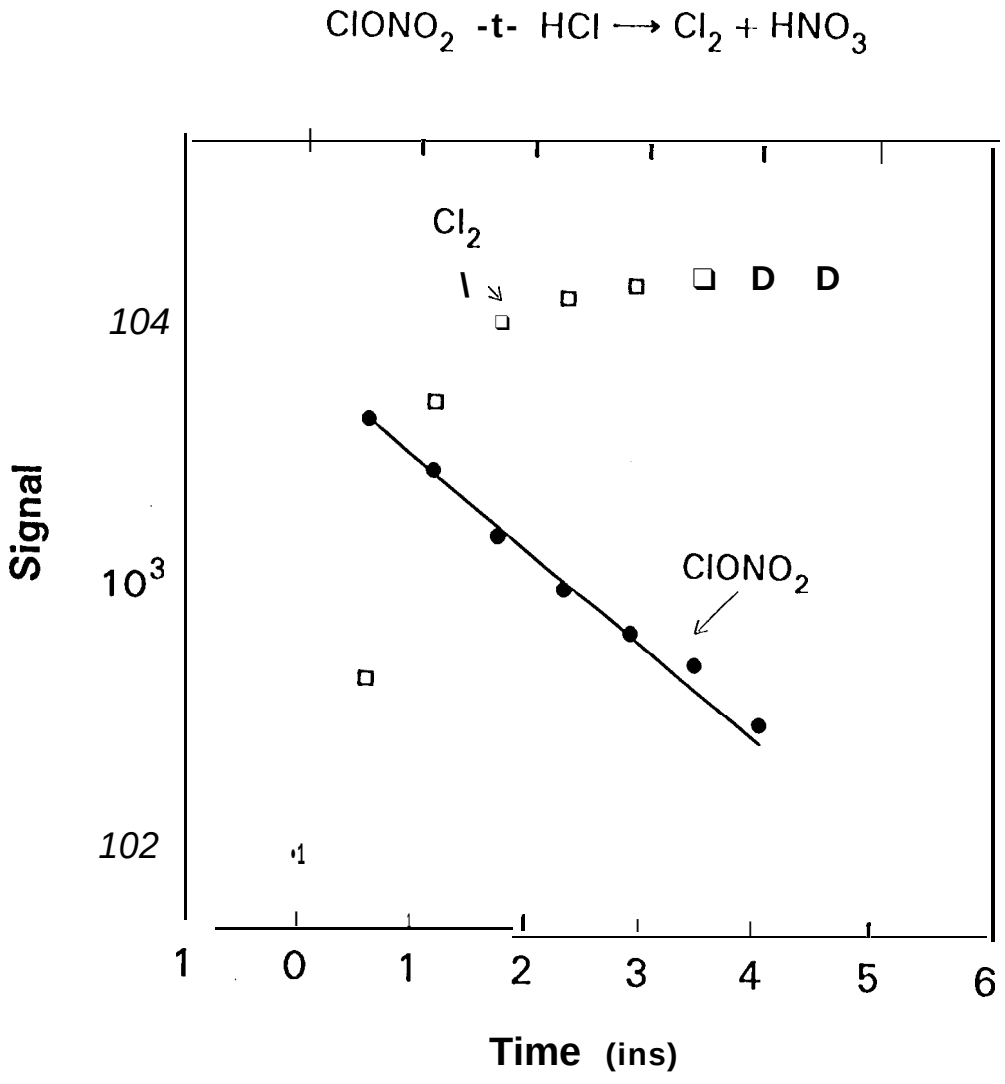

GCLONOIL.SP5

Figure 3

$$ClONO_2 + HCl \longrightarrow Cl_2 \text{ -t- } HNO_3$$

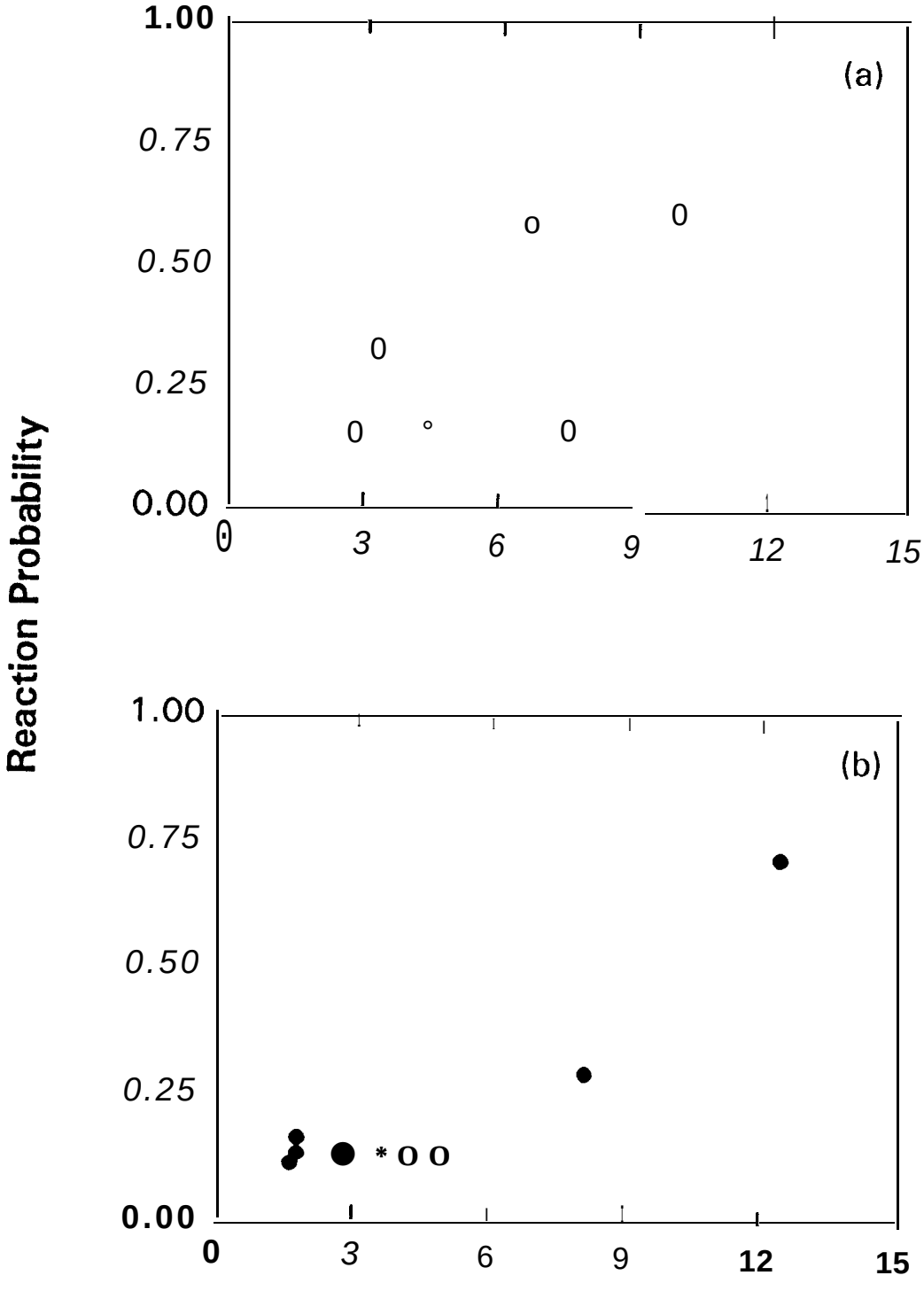

Figure 4 (a), (b)

CIONSEP1.SP5

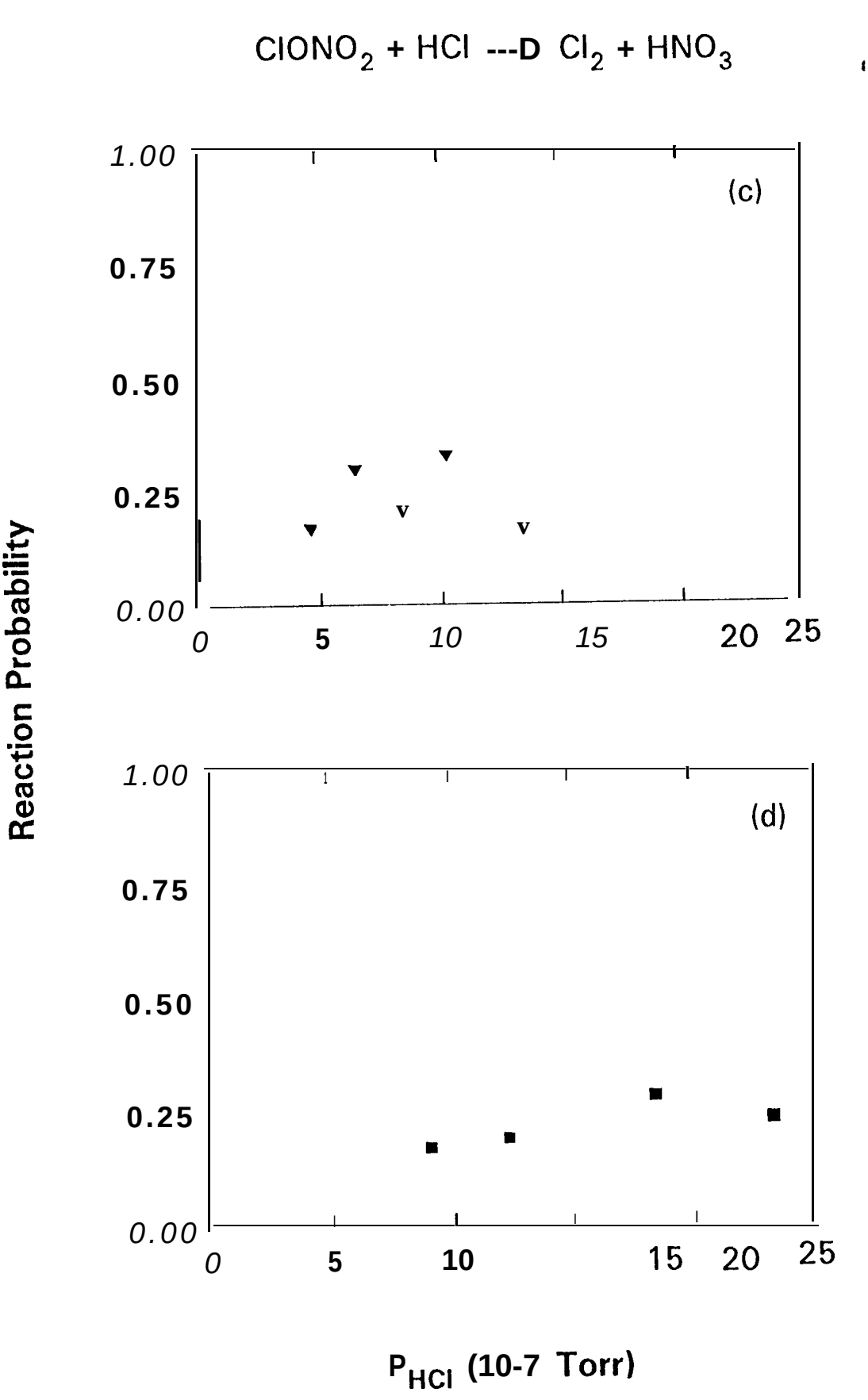
ClONO2 + HCl ---D Cl2 + HNO3
Reaction Probability
1.00
0.75
0.50
0.25
0.00
(c)
0
5
10
15
20
25
1.00
0.75
0.50
0.25
0.00
(d)
0
5
10
15
20
25
PHCl (10-7 Torr)

Figures 4(c), (d)

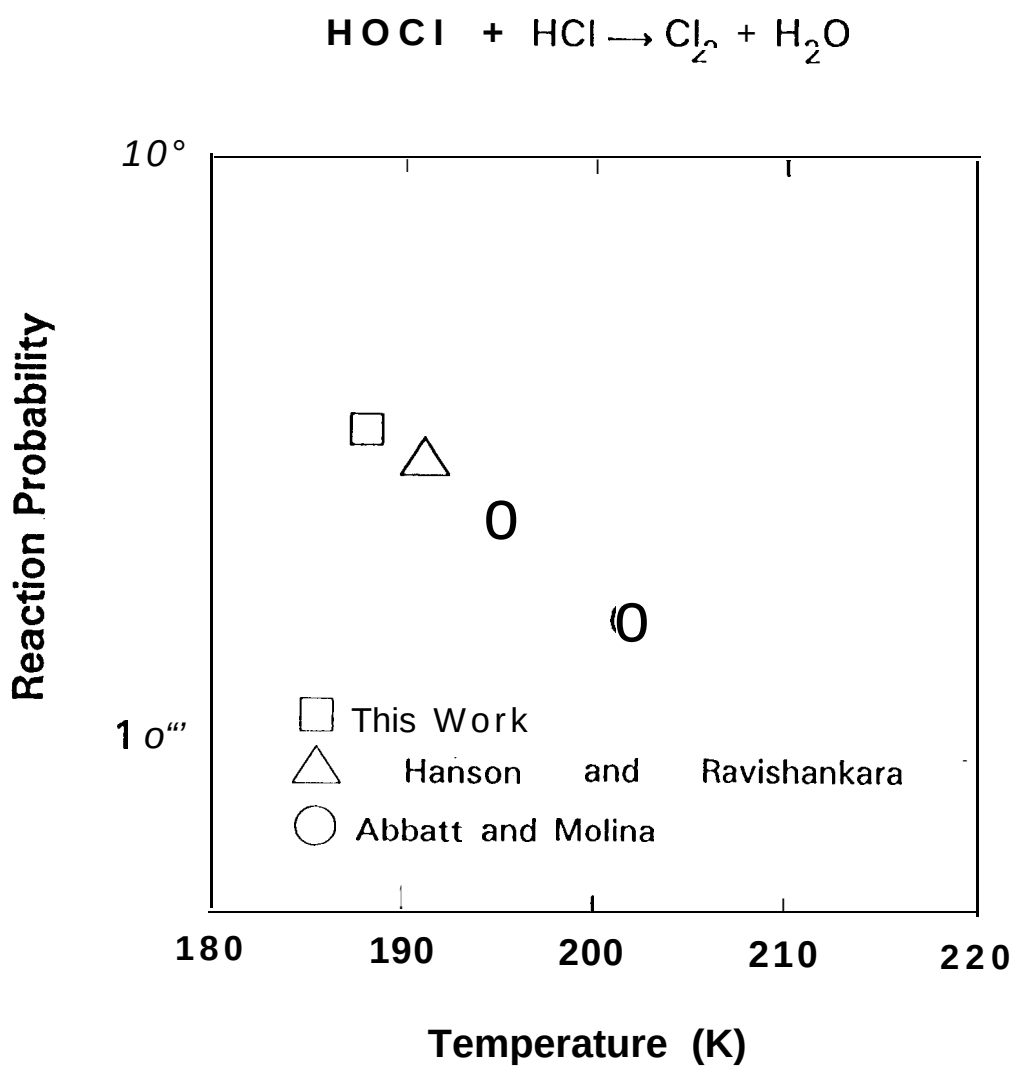

Figure 5

HOClComp.SP5

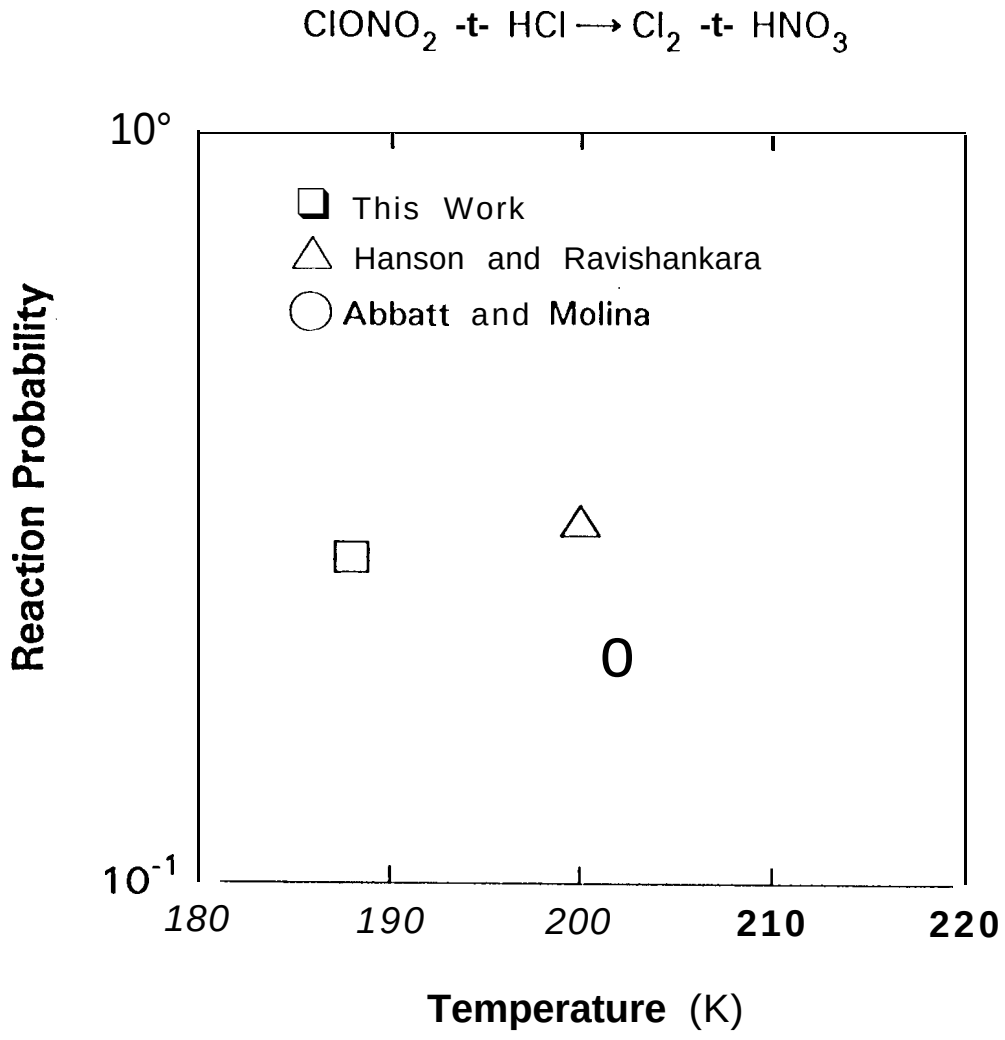
ClONO2 -t- HCl ⟶ Cl2 -t- HNO3
10°
10-1
This Work
Hanson and Ravishankara
Abbatt and Molina
Reaction Probability
180
190
200
210
220
Temperature (K)

Figure 6